BIOLOGY OF REPRODUCTION **76,** 353–361 (2007)
Published online before print 22 November 2006.
DOI 10.1095/biolreprod.106.056887

Semen-Coagulating Protein, SVS2, in Mouse Seminal Plasma Controls Sperm Fertility[1]

Natsuko Kawano and Manabu Yoshida[2]

Misaki Marine Biological Station, Graduate School of Science, The University of Tokyo, Kanagawa 238-0225, Japan

ABSTRACT

Mammalian seminal plasma is known to contain a decapacitation factor(s) that prevents capacitation and thus, the fertility of sperm. This phenomenon has been observed in experiments conducted in vitro that assessed the inhibition of epididymal sperm fertility by seminal plasma or by the purified decapacitation factor. However, the phenomenon of decapacitation has not yet been characterized in vivo. In the present study, we demonstrate that seminal vesicle protein secretion 2 (SVS2), which is a 40-kDa basic protein and a major component of the copulatory plug, enters the uterus and interacts with ejaculated sperm heads after copulation. The SVS2-binding region of sperm changed from the postacrosomal region to the equatorial segment, while the sperm migrated through the uterus and finally disappeared in the oviduct. Furthermore, SVS2 reduced the fertility of epididymal sperm. The sperm treated with SVS2 decreased the percentage of fertilized oocytes from 60% to 10%. The capacitation state was assessed by protein tyrosine phosphorylation and the comprehensiveness of the acrosome reaction. SVS2 functioned to maintain sperm in the uncapacitated state and to reverse capacitated sperm to the uncapacitated state. We found that the fertility of ejaculated sperm is associated with SVS2 distribution in the female reproductive tract. These results indicate that SVS2 functions as a decapacitation factor for mouse sperm.

acrosome reaction, decapacitation factor, epididymal sperm, female reproductive tract, fertilization, male reproductive tract, seminal vesicles, sperm capacitation

INTRODUCTION

Mammalian sperm are incapable of fertilizing oocytes immediately after ejaculation. Ejaculated sperm gain fertility after remaining in the female reproductive tract for an appropriate time period [1, 2]. The term for this time-dependent acquisition of fertility is sperm capacitation; capacitated sperm undergo the acrosome reaction, penetrate the zona pellucida, and eventually bind and fuse with oocytes. Although the molecular mechanism underlying sperm capacitation is poorly understood, many studies involving the use of epididymal sperm have revealed that capacitation is correlated with changes in the fluidity of the sperm plasma membrane, intracellular ion concentration, metabolism, tyrosine phosphorylation of sperm proteins, and motility [3–6].

On the other hand, as shown by Chang in 1957 [7], capacitated sperm reversibly lose their capacitated state when treated with seminal plasma [7]. This phenomenon is known as the decapacitation of spermatozoa [8], and the decapacitation factor in the seminal plasma appears to be conserved among several species [7]. Subsequent to this finding, many studies have focused on identifying the decapacitation factor in seminal plasma using several in vitro assays; however, this factor has remained obscure. For example, in the rabbit, three discrepant molecules have been identified as decapacitation factors, including a peptide [9], cholesterol-containing vesicles [10], and a protein [11]. Recently, three separate studies have variously identified the mouse decapacitation factor as a 40-kDa anionic polypeptide [12], a 19-kDa glycoprotein [13], and phosphatidylethanolamine-binding protein 1 [14]. However, a decapacitation factor that is common to several species has not yet been described. Moreover, since the decapacitation effect of seminal plasma has been observed only in vitro, it is unclear whether the inhibitory mechanism of sperm fertility actually exists in the female reproductive tract after copulation.

In most mammalian species, a common characteristic of seminal plasma is the formation of a coagulum [15]. In humans, semen coagulum is known to be synthesized from semenogelin (SEMG) secreted from the seminal vesicle [16]. This protein is a member of the gene family that encodes semen-coagulating proteins found in many species, such as several types of primates [17], mice [18], rats [19], and pigs [20–22]. Furthermore, SEMG is known to be a native regulator of sperm fertility and motility. Upon treatment with fetal cord serum ultrafiltrate, SEMG protects human sperm from protein tyrosine phosphorylation and prevents induction of the acrosome reaction [23]. Yoshida and coworkers [24] have reported that the motility of ejaculated sperm correlates with the SEMG concentration in ejaculated human semen. These findings suggest that the members of this gene family act as decapacitation factors.

In mice, the copulatory plug is formed by semenoclotin, seminal vesicle secretion 2 protein (SVS2) [18]. SVS2 consists of 375 amino acids, has a molecular mass of 40 kDa, and is a member of the semen-clotting protein family. It shows 55% similarity to human SEMG in the 55 amino acids of the N-terminal region that contains a signal peptide (Fig. 1A, solid box). Both SVS2 and SEMG are rich in lysine (SVS2, 10.4%; SEMG, 8.9–10.0%) and are highly basic proteins (pI values of 10.68 for SVS2 and 9.45–9.68 for SEMG). Considering these similarities, it is possible that SVS2 has an inhibitory effect on sperm fertility, although it is known that SVS2 acts as a substrate for transglutaminase to form the copulatory plug.

In the present study, to elucidate the phenomenon of decapacitation in vivo, we examined the effects of SVS2 on mouse sperm fertility and the interaction between SVS2 and sperm in the female reproductive tract after copulation. The experiments were conducted in mice, which serve as a convenient model for observing in vivo phenomena and studying the inhibition of sperm fertility.

[1]Supported by Grants-in-Aid 16687003 and 17049014 to M.Y. from the Ministry of Education, Culture, Sports, Science and Technology of Japan.
[2]Correspondence: FAX: 81 46 881 7944;
e-mail: yoshida@mmbs.s.u-tokyo.ac.jp

Received: 29 August 2006.
First decision: 11 September 2006.
Accepted: 31 October 2006.

ISSN: 0006-3363. http://www.biolreprod.org

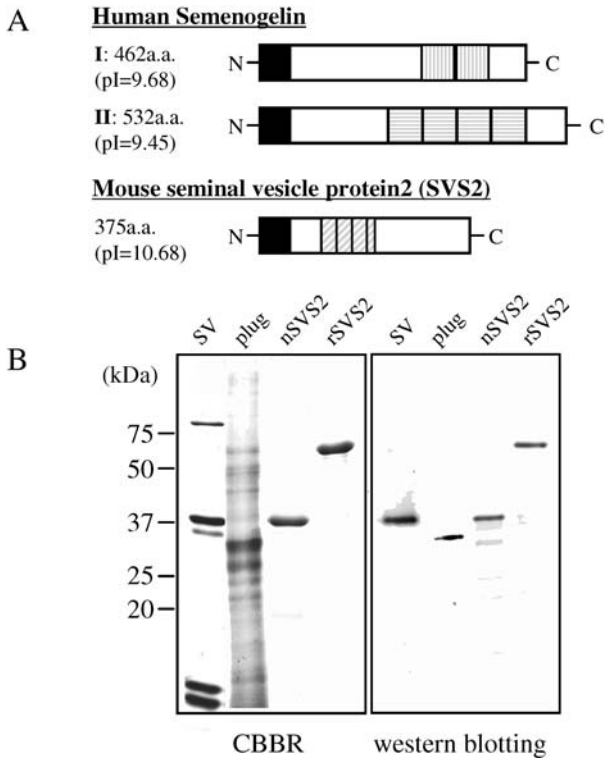

FIG. 1. **A**) Protein structures of mouse SVS2 and human SEMG constructed from the amino acid sequences described previously [16, 18]. The solid boxes show the highly conserved regions, and the gray boxes show the repeat regions. **B**) SDS-PAGE of the mouse seminal vesicle fluid (SV), copulatory plug (plug), purified seminal vesicle fluid (nSVS2), and GST-tagged recombinant SVS2 (rSVS2), which was followed by Coomassie Brilliant Blue R250 (CBBR) staining and Western blotting using the anti-SVS2 antibody. SVS2 is detected as a 40-kDa protein in SV and nSVS2 and as a 30-kDa protein in the plug, while rSVS2 is observed as a 65-kDa protein, since it is fused with GST.

MATERIALS AND METHODS

Preparation of Native and Recombinant SVS2

All experiments were performed with the approval of the Animal Care Committee of the University of Tokyo. Seminal vesicles were isolated from 9- to 13-wk-old male mice (CD-1; Charles River Japan Yokohama) by dissection, and the fluids from these vesicles were collected. This seminal vesicle fluid was dissolved in PBS (pH 7.5) and centrifuged at 10 000 × *g* for 10 min at 4°C. The supernatant was separated using a gel filtration column (1 × 50 cm; Bio-Gel P-30; Bio-Rad Japan, Tokyo) in PBS, and a protein of approximately 40-kDa was isolated as the native SVS2 (nSVS2). Following desalination and lyophilization, purified nSVS2 was stored at −20°C until use.

The cDNA that encodes *SVS2* (NCBI accession number X91270) was prepared by reverse transcriptase-PCR using the RNA isolated from mouse seminal vesicles. In order to prepare the GST-tagged recombinant protein of full-length SVS2, the *svs2* cDNA was subcloned into pGEX-6p-1 (GE Healthcare, Buckinghamshire, UK). The GST-SVS2 fusion protein was produced in *Escherichia coli* BL21-pLysS by inducing with 1 mM isopropyl b-D(–)-thiogalactopyranoside. After lysis of *E. coli* by sonication, the sample was centrifuged (12 000 × *g* for 30 min) and the supernatant was discarded. The precipitate was dissolved in 4% (v/v) Triton X-100, followed by two washes with MilliQ water for 30 min. The insoluble fraction was then lysed in 8 M urea with shaking for 1 h at 37°C, and subsequently centrifuged at 4°C (12 000 × *g* for 30 min). The supernatant that contained the recombinant SVS2 (rSVS2) was desalted using PD-10 columns (GE Healthcare) and was purified by affinity chromatography on glutathione–Sepharose 4B (GE Healthcare), according to the suppliers instructions.

Preparation of Mouse Sperm

Epididymal sperm were collected from 9- to 13-wk-old male mice (C57BL/6J; Charles River Japan) and capacitated in HS medium (135 mM NaCl, 5 mM KCl, 1 mM $MgCl_2$, 2 mM $CaCl_2$, 30 mM Hepes, 10 mM glucose, 10 mM lactic acid, 1 mM pyruvic acid, 5 mg/ml BSA, 15 mM $NaHCO_3$, [pH 7.4]) at 37°C under 5% CO_2 as described previously [25].

The ejaculated sperm were collected in the following manner. Female mice aged 8 to 19 wks were mated with 9- to 13-wk-old males. Subsequently, the female mice were killed, and their reproductive tracts were separated into the following parts: the oviduct, the uterine region near the oviduct, the uterine region near the cervix, and the vagina. The contents of each part were obtained by flushing the tract with 1 ml PBS. The contents were then centrifuged at 2000 × *g*, and the sperm pellets from each part were collected. In order to examine the number and motility of the sperm in the female reproductive tract after copulation, we collected the sperm at 0, 1, 2, and 3 h after copulation. To evaluate the sperm fertility and sperm-SVS2-binding status, sperm were collected 3 h after copulation when the first sperm were observed in the oviduct.

In Vitro Fertilization

Epididymal sperm were suspended in HS medium with or without 25 μM nSVS2/rSVS2, 1 mg/ml casein, and 1 mg/ml RNase (Type I-AS from bovine pancreas; Sigma-Japan, Tokyo), and were then incubated for 90 min at 37°C in an atmosphere of 5% CO_2. Mature oocytes were collected by superovulation treatment [26], and the cumulus cells were removed by incubation with 0.01% (w/v) hyaluronidase (Sigma-Japan) in HS medium. Pre-incubated sperm were added to the cumulus-free oocytes at a final concentration of 1–1.5 × 10^5 cells/ml. After 6 h of incubation, the oocytes were fixed with 2% (w/v) paraformaldehyde, and then stained with 100 ng/ml DAPI, to facilitate observations of sperm nuclei in the oocyte cytoplasm.

Western Blot Analysis

Production of rabbit antiserum against purified nSVS2 was performed by Operon Biotechnologies (Tokyo), and the anti-SVS2 polyclonal antibody was purified by affinity column chromatography (HiTrap Protein A; GE Healthcare).

The supernatants of the contents from each part of the female reproductive tract were precipitated with acetone and dissolved in SDS-PAGE sample buffer. The proteins were separated by Tricine SDS-PAGE using a 16% polyacrylamide gel and transferred onto a PVDF membrane (Millipore). The membrane was blocked using 5% (w/v) blocking agent (GE Healthcare) in TBS with 0.1% Tween 20 (TBS-T) and then incubated for 3 h at room temperature with 20 μg/ml of the anti-SVS2 antibody in TBS-T that contained 5% (w/v) BSA. After washing with TBS-T, the membrane was treated with HRP-conjugated anti-rabbit IgG (Wako, Japan) at a dilution of 1:10 000 in TBS-T for 1 h at room temperature and visualized with the ECL Plus Western blotting detection system (GE Healthcare). Densitometric analysis of Coomassie Brilliant Blue R250 (CBBR) staining was performed with a computer image analysis program (ImageJ version 1.32j).

In order to detect tyrosine phosphorylation of the sperm proteins, the sperm were incubated with or without nSVS2 for 0–3 h at 37°C in an atmosphere that contained 5% CO_2, and were then dissolved in SDS-PAGE sample buffer (1 × 10^7 cells/ml). These samples were separated by SDS-PAGE using a 12% polyacrylamide gel and analyzed by Western blotting using anti-phosphotyrosine antibody (Upstate Biotechnology Inc., Lake Placid, NY) at a 1:5000 dilution. After treating with anti-mouse IgG (Kirkegaard & Perry Laboratories, Inc., Gaithersburg, MD) at a 1:10 000 dilution, the phosphotyrosine signals were visualized as described above.

Acrosome Reaction Assay

Epididymal sperm were incubated with HS medium that contained nSVS2/rSVS2 for 3 h at 37°C in an atmosphere that contained 5% CO_2, and were treated with 15 μM ionomycin for 10 min at room temperature or with 100 μM progesterone (Wako) at 37°C for 15 min. The ejaculated sperm were also treated with ionomycin or progesterone immediately after they were collected from the female reproductive tract. The acrosome-reacted sperm were assessed by staining with FITC-conjugated *Arachis hypogaea* lectin (PNA lectin; Sigma) according to the previously described method [27].

Localization of SVS2 in Sperm

nSVS2 was conjugated with Alexa 594 using the Alexa Fluor 594 protein-labeling kit (Invitrogen Japan KK, Tokyo). Alexa 594-conjugated nSVS2 was added to the epididymal sperm suspension at a final concentration of approximately 2.5 μM, and the suspension was incubated at 37°C for 1 h in an atmosphere of 5% CO_2. The sperm were washed twice, fixed with 2%

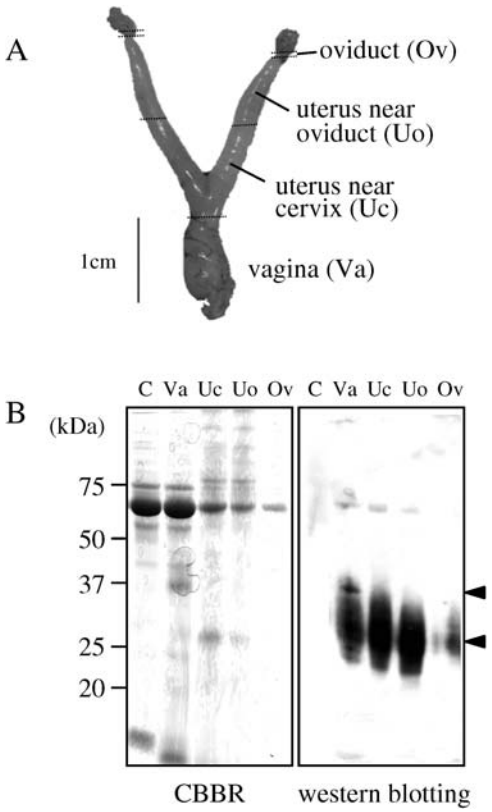

FIG. 2. Organization of the female reproductive tract (**A**) and SVS2 distribution in the female reproductive tract after copulation (**B**). **A**) The reproductive tracts of female mice were separated into the vagina (Va), uterine region near the cervix (Uc), uterine region near the oviduct (Uo), and oviduct (Ov). **B**) Ejaculated semen collected from each part of the reproductive tract of females postcoitus were subjected to SDS-PAGE, followed by CBBR staining and Western blotting using the anti-SVS2 antibody. After copulation, each part of the female reproductive tract contains the SVS2 signal, while no signal is detected in the entire reproductive tract of virgin female mice (C). In Va, Uc and Uo, a broad band is detected at approximately 22–30 kDa by Western blotting.

paraformaldehyde, and then observed under a fluorescent microscope (IX-71; Olympus) equipped with a U-MWIG2 mirror unit (Olympus).

Epididymal sperm pretreated with SVS2 or ejaculated sperm were incubated with 20 μg/ml of the anti-SVS2 antibody in PBS that contained 2% (w/v) Block Ace (Dainippon Pharmaceutical, Tokyo, Japan) for 3 h. The samples were washed twice with PBS and incubated with the Alexa 488-conjugated anti-rabbit antibody (Invitrogen; diluted 1:500) for 1 h. After washing twice, the samples were fixed with 2% (w/v) paraformaldehyde and observed with a fluorescent microscope equipped with a U-MNIBA2 mirror unit (Olympus).

Statistical Analysis

Data are expressed as means ± SEM. The probability of statistically significant data was calculated using the chi-square test and Student *t*-test. Data with $P < 0.01$ are indicated by asterisks in Figures 3 and 4.

RESULTS

SVS2 in Mouse Seminal Vesicles and Copulatory Plugs

It is known that SVS2 is a 40-kDa protein that is found in the seminal vesicle fluid [18]. We first purified SVS2 from the seminal vesicle fluid (nSVS2). Five major proteins were found in the seminal vesicle fluid, and the anti-nSVS2 polyclonal antibody cross-reacted only with the 40-kDa protein (Fig. 1B). Moreover, recombinant SVS2 (rSVS2) synthesized in *E. coli* as a GST-fusion protein was recognized by the anti-SVS2 antibody as a 65-kDa protein. The difference in the molecular masses of rSVS2 and nSVS2 reflects the attachment of the GST-tag to these proteins (Fig. 1B). It is known that after copulation, the major portion of SVS2 is cross-linked by transglutaminase produced by the prostate and forms a vaginal plug [15]. In the present study, smeared multiple bands were observed in SDS-PAGE of the copulatory plug, and a band of approximately 30 kDa reacted with the anti-SVS2 antibody in Western blots.

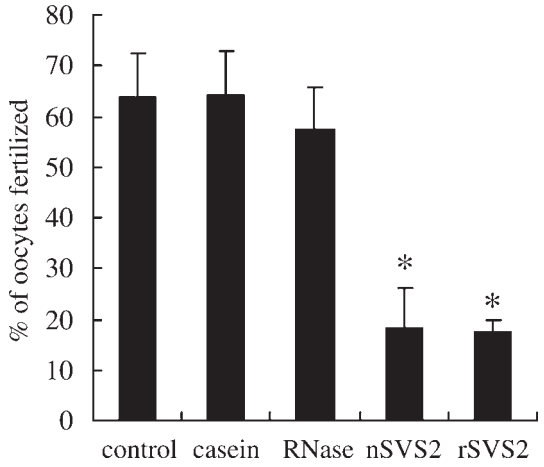

FIG. 3. *In vitro* fertilization of cumulus-free mouse oocytes with epididymal sperm incubated with or without 25 μM nSVS2/rSVS2. Epididymal sperm were preincubated in the medium with or without 25 μM nSVS2/rSVS2 for 90 min before coincubation with oocytes. Fertilized oocytes that contained sperm heads were identified by DAPI staining. The data represent the mean ± SEM of three independent experiments. Asterisks indicate significant differenced from control sperm at $P < 0.01$ by the chi-square test.

SVS2 in the Female Reproductive Tract after Copulation

It is known that the copulatory plug prevents the fertilization of a recently inseminated female by rival males during subsequent copulations [17]. However, no information is available regarding the presence of SVS2 in the uterus. To clarify whether SVS2 enters the uterus, we collected the contents from the following parts of the female reproductive tract 3 h after copulation: the vagina, the uterine region near the cervix, the uterine region near the oviduct, and the oviduct (Fig. 2A). These contents were separated by Tricine SDS-PAGE and analyzed by Western blotting with the anti-SVS2 antibody (Fig. 2B). SVS2 signals were detected in the contents of each part of the female reproductive tract, while no signal was detected in the reproductive tract of a virgin female. In the contents collected from the vagina and the two uterine regions after copulation, a broad band of approximately 22–30 kDa and a band of 40 kDa were detected by Western blotting (Fig. 2B, arrowheads). A similar phenomenon has been observed in humans: SEMG is degraded by the serine protease termed prostate-specific antigen (PSA), which is secreted from the prostate in the ejaculated semen [28]. It is possible that the intact 40-kDa SVS2 was degraded to approximately 22–30 kDa by PSA after copulation. The 22–30-kDa broad band obtained from the uterus appeared to be larger than that obtained from the vagina, while the SVS2 signal detected in the oviduct was very weak (Fig. 2B). Therefore, the plug-forming SVS2 enters the uterus and may have some effect on sperm functions. The protein concentration of the uterus was approximately 7 mg/ml, and densitometry analysis showed

that SVS2 accounted for 15% of the total protein. Accordingly, the physiological concentration of SVS2 was defined as 25 μM, and we used SVS2 at this concentration in all the subsequent in vitro experiments.

Effects of SVS2 on Sperm Fertility In Vitro

To examine the effect of SVS2 on epididymal sperm fertility, we investigated the two types of SVS2 protein (nSVS2 and rSVS2) using in vitro fertilization assays. When the epididymal sperm were incubated and used to inseminate oocytes, 57.6 ± 8.7% (n = 69 in three batches) were fertilized. In contrast, when sperm were treated with 25 μM nSVS2 or rSVS2, the fertilization rate decreased to 10.7 ± 2.5% (n = 60 in 3 batches) and 17.5 ± 3.5% (n = 65 in 3 batches), respectively (Fig. 3). As a negative control, the addition of casein and RNase to the medium at a concentration of 1 mg/ml did not affect sperm fertilizing capability. These results indicate that SVS2 inhibits epididymal sperm fertility.

Effects of SVS2 on Sperm Capacitation

To investigate the mechanism of SVS2-dependent sperm fertility inhibition, we examined the effect of SVS2 on epididymal sperm capacitation using the following two characteristics: a capacitation-specific increase in protein tyrosine phosphorylation [5], and induction of the acrosome reaction depending on capacitation state [29, 30]. Western blotting using the anti-phosphotyrosine antibody revealed tyrosine phosphorylation of the 116-, 70-, 55-, 45-, 40-, 30-, and 28-kDa proteins in epididymal sperm. With regard to these proteins, tyrosine phosphorylation of the 70-, 55-, 45-, 40-, and 28-kDa proteins increased continuously during the 3-h incubation in HS medium, as shown previously [5] (Fig. 4A).

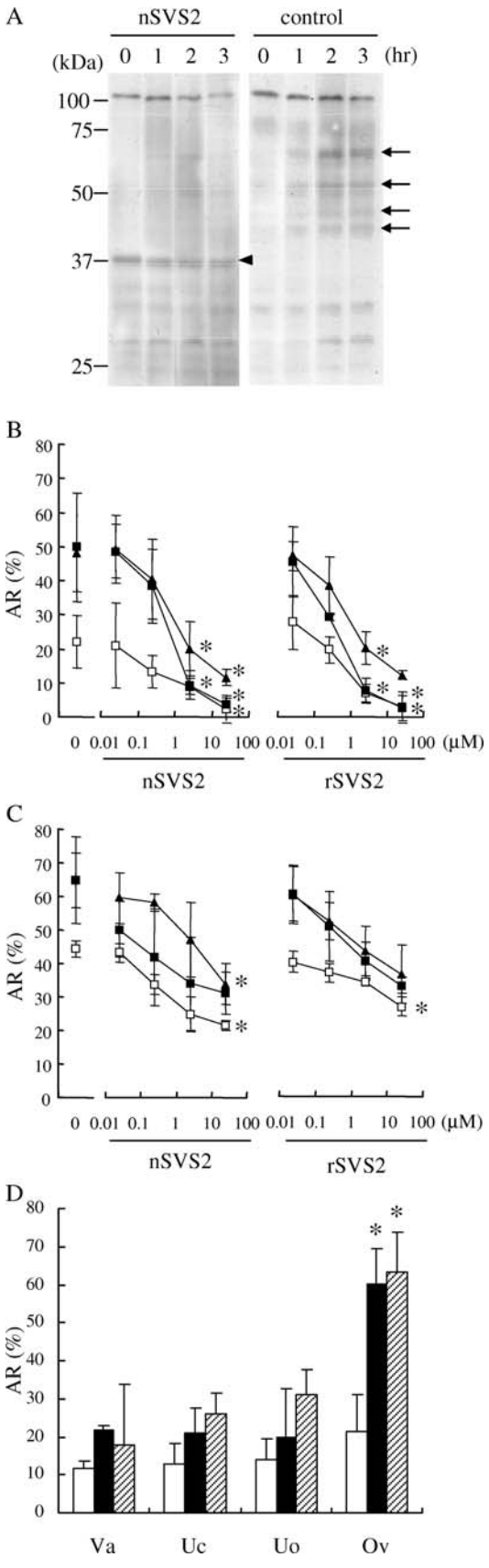

FIG. 4. The effect of SVS2 on sperm capacitation. **A**) Increased protein tyrosine phosphorylation. Epididymal sperm were incubated with or without 25 μM nSVS2 for 3 h, followed by SDS-PAGE and Western blotting using the anti-phosphotyrosine antibody. As indicated by the arrows, the 70-, 55-, 45-, and 40-kDa proteins appear to increase in the control sperm, but not in the 25-μM nSVS2-treated sperm. In the lanes with nSVS2-treated sperm, a 40-kDa nSVS2 protein is detected by the nonspecific binding of antibodies (arrowhead). This blot is representative of at least five experiments. **B**) The acrosome reaction induced by ionomycin and progesterone in sperm treated with nSVS2/rSVS2 at concentrations that ranged from 0 μM to 25 μM. After the incubation of epididymal sperm with or without nSVS2/rSVS2 for 3 h, they were either not treated at all (white squares) or were treated with ionomycin (black triangle) or progesterone (black square). The acrosome reactions induced by these drugs were estimated by FITC-PNA staining. Each bar represents the mean ± SEM of three experiments. A minimum of 200 sperm was counted for each of the assays. Asterisks indicate significant differences ($P < 0.01$, Student *t*-test) between the acrosome reaction rates of nSVS2- or rSVS2-incubated sperm and the corresponding control sperm. **C**) The effect of SVS2 on capacitated sperm. After 3 h of incubation of epididymal sperm without SVS2, they were incubated with or without nSVS2/rSVS2 at concentrations that ranged from 0 μM to 25 μM for 1 h. Following treatment with nothing (white square), ionomycin (black triangle), and progesterone (black square), the numbers of acrosome-reacted sperm were estimated. **D**) Acrosome reactions in the ejaculated sperm. The capacitation statuses of the ejaculated sperm collected from each part of the female reproductive tract were assessed by treatment with nothing (open bar), ionomycin (filled bar), and progesterone (hatched bar). Va, vagina; Uc, uterine region near the cervix; Uo, uterine region near the oviduct; Ov, oviduct. Each bar represents the mean ± SEM of five experiments. A minimum of 50 sperm was counted for each assay. Asterisks indicate significant differences ($P < 0.01$, Student *t*-test) compared with the acrosome reaction of ejaculated sperm collected from other parts of the female reproductive tract.

However, in the nSVS2-treated sperm, tyrosine phosphorylation of the 70-, 55-, 45-, and 40-kDa proteins was only slightly increased during the incubation period (arrows in Fig. 4A). In the lanes with nSVS2-treated sperm, a 40-kDa nSVS2 band was detected by nonspecific binding of the anti-phosphotyrosine antibody (arrowheads in Fig. 4A). The increase in tyrosine phosphorylation of the 25 μM rSVS2-treated sperm was also inhibited during the 3-h incubation (data not shown).

Next, we measured the acrosome reaction induced by ionomycin and progesterone; these drugs increase the $[Ca^{2+}]_i$ of sperm, and capacitated sperm can undergo the acrosome reaction [25, 31]. As shown in Figure 4B, both ionomycin and progesterone induced the acrosome reaction in epididymal sperm treated without SVS2 (42 ± 6.4% [n = 298] and 40.5 ± 2.1% [n = 291], respectively). In contrast, these acrosome reactions were inhibited in a dose-dependent manner when the sperm were pretreated with nSVS2 or rSVS2 ($P < 0.01$). Spontaneous acrosome reaction by noninducers was also dose-dependently prevented by treatments with nSVS2 and rSVS2 (Fig. 4B). Furthermore, we examined the inhibitory effect of SVS2 on fully capacitated sperm. When the 3-h incubated sperm were additionally incubated with 0–25 μM nSVS2 or rSVS2 for 1 h, ionomycin- and progesterone-induced acrosome reactions decreased dose-dependently compared with sperm that were not treated with either nSVS2 or rSVS2. At a concentration of 25 μM nSVS2/rSVS2, the spontaneous acrosome reactions were maintained at about 20% (Fig. 4C), as well as that of the control sperm prior to the additional incubation (Fig. 4B). These results show that SVS2 inhibits the induction of both capacitation and the spontaneous acrosome reaction and also reverses the sperm capacitation status.

In order to determine the capacitation state of ejaculated sperm in the female reproductive tract, we collected sperm from four parts of the reproductive tract at 3 h postcoitus, and examined the sperm for the acrosome reaction induced by identical treatments with ionomycin or progesterone. The sperm in the oviducts showed approximately three-fold higher responses to ionomycin (60.2 ± 9.2%, n = 185 in 3 batches) and progesterone (63.3 ± 10.4%, n = 167 in 3 batches) than sperm treated without these inducers (21.3 ± 9.9%, n = 165 in 3 batches) (Fig. 4C). On the other hand, sperm from the other parts of the female reproductive tract, i.e., the vagina, the uterine region near the cervix, and the uterine region near the oviduct, did not show significant responses to these drugs (Fig. 4C). These results suggest that the ejaculated sperm were capacitated in the oviduct but not in the vagina or the uterus. Therefore, SVS2 appears to inhibit premature sperm capacitation and to preserve the capacitated sperm status until the sperm reach the oviduct.

Patterns of SVS2 Binding to Epididymal Sperm

We observed the interaction of fluorescence-conjugated SVS2 with epididymal sperm, in order to examine whether SVS2 binds to the sperm surface. When epididymal sperm were stained with Alexa 594-labeled SVS2, a strong fluorescence signal was detected in the postacrosomal region of the sperm head (Fig. 5A). No signal was detected when epididymal sperm were treated with Alexa 594 alone (data not shown). However, when the sperm were pretreated with 25 μM nSVS2 before staining with labeled SVS2, a strong signal in the postacrosomal region was not observed (Fig. 5B). This shows that SVS2 that is prebound to the postacrosomal region interferes with the interaction between the sperm surface and Alexa 594-labeled SVS2, and that Alexa 594-SVS2 specifically binds to the postacrosomal region. Alexa 594-SVS2 was also bound to the entire regions of the sperm head and flagella in both treatments (Fig. 5, A and B), which indicates that the fluorescent signals in the acrosomal and flagellar regions are nonspecific.

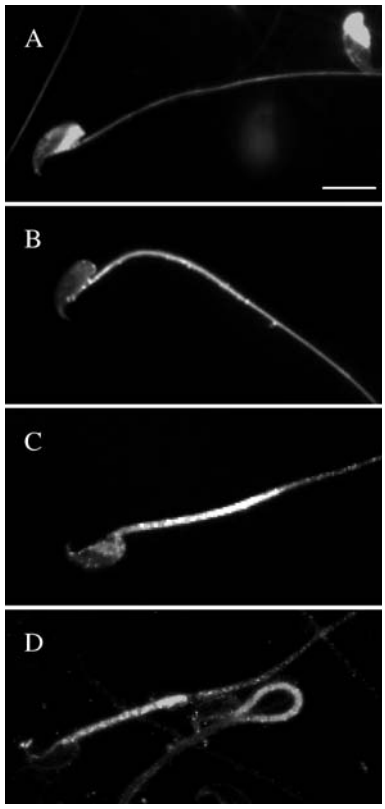

FIG. 5. Interaction between SVS2 and the epididymal sperm surface was detected using SVS2 conjugated with Alexa 594 (**A**, **B**) and by immunostaining with the anti-SVS2 antibody (**C**, **D**). **A**) Typical fluorescence pattern of sperm treated with Alexa 594-conjugated SVS2. In general, the postacrosomal region is stained. **B**) Sperm treated with nSVS2 before incubation with the Alexa 594-conjugated SVS2. The fluorescence in the postacrosomal region has disappeared. **C**) Immunostaining with the anti-SVS2 antibody of sperm incubated with nSVS2. A pronounced signal is localized in the postacrosomal region. **D**) Immunostaining using the anti-SVS2 antibody of sperm not treated with SVS2. Almost no fluorescence is observed in the sperm head, whereas a nonspecific signal is detected in the entire sperm surface. All the photographs were obtained after the same exposure time in order to display the differences in brightness observed using a 60× objective lens. Bar = 5 μm.

Similar results were obtained for the immunostaining of epididymal sperm with the anti-SVS2 antibody. Immunostaining with anti-SVS2 antibody of epididymal sperm pretreated with 25 μM nSVS2 showed signals overall and a pronounced signal in the postacrosomal region (Fig. 5C). However, the sperm collected from the epididymis did not show any signals in the postacrosomal region of the sperm head (Fig. 5D). Regardless of SVS2 treatment, immunostaining with anti-SVS2 antibody showed a weak signal overall and a strong signal in the midpiece (Fig. 5, C and D). These results indicate that SVS2 binds specifically to the postacrosomal region of epididymal sperm, although it binds nonspecifically to the entire sperm surface.

Transition of the SVS2-Binding Pattern of Sperm in the Female Reproductive Tract

To elucidate the in vivo effect of SVS2 on sperm, we examined the SVS2-binding patterns of ejaculated sperm.

TABLE 1. The proportion of the SVS2-binding patterns of ejaculated sperm in the following four parts of the female reproductive tract; vagina, the uterine region near the cervix, the uterine region near the oviduct, and oviduct.

Location of ejaculated sperm	n*	Staining patterns† (%)			
		Dispersed	Postacrosome	Band	No-binding
Oviduct	32	6.3	0	15.6	78.1
Uterine region near the oviduct	53	9.4	18.9	71.7	0
Uterine region near the cervix	55	10.9	63.6	25.5	0
Vagina	52	80.8	19.2	0	0

* n = The number of total sperm obtained from 5 experiments.
† SVS2-binding patterns described in Figure 6 A–D.

Ejaculated sperm were collected from each part of the female reproductive tract and immunostained with the anti-SVS2 antibody. Variations were observed in the SVS2-binding patterns of the sperm in the different parts of the female reproductive tract. The proportions of the SVS2-binding patterns of the sperm from each part of the female reproductive tract are shown in Table 1. In the vagina, the copulatory plug occupied most of the space, and few nonmotile sperm were found (data not shown). This result supports the assumption that mouse semen is ejaculated directly into the uterus [4, 32]. Immunostaining experiments revealed that a large proportion (80.8%) of the sperm in the vagina did not exhibit a specific signal for SVS2 binding, although a faint signal was detected in the entire head region (Fig. 6A). This phenomenon may be similar to the nonspecific staining patterns observed for epididymal sperm (see Fig. 5D). In the uterus, almost all the ejaculated sperm were present for 0–3 h after copulation and showed very high motility. Immunostaining of the sperm in the uterine region near the cervix showed that approximately 60% of the sperm exhibited a specific signal in the postacrosomal region (Fig. 6B). This pattern was in accordance with that of epididymal sperm incubated with SVS2 in vitro (Fig. 5, A and C). In the uterine region near the oviduct, the SVS2 signal was observed mainly in the equatorial segment of the sperm head (Fig. 6C). The proportion of sperm that exhibited this binding pattern was 71.7%, which suggests that the SVS2-binding region of the sperm had shifted from the postacrosomal region to the equatorial segment. Finally, the sperm appeared in the oviduct at 3 h postcoitus, and they appeared to be hyperactivated and aggregated around the oocytes and oviductal tissue. Almost all of the ejaculated sperm in the oviduct lacked SVS2 signals (Fig. 6D). These results suggest that SVS2 binds to the sperm surface and is released when the sperm become capacitated and hyperactivated.

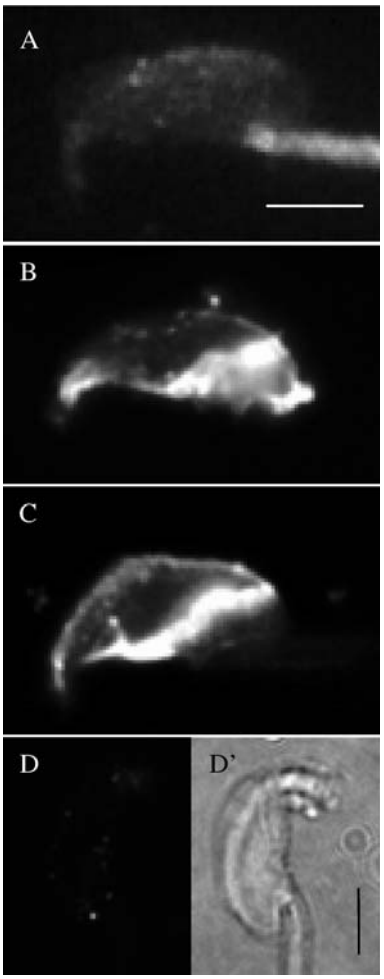

FIG. 6. The SVS2-binding patterns of ejaculated sperm in the female reproductive tract. The ejaculated sperm were collected from four different parts of the female reproductive tract and were subjected to immunostaining using the anti-SVS2 antibody. As shown in Table 1, the staining patterns are categorized into dispersed (**A**), postacrosome (**B**), band (**C**), and no-binding (**D**). **D'**) Bright-field image of **D**. These photos are representative results of five independent experiments. Bar = 2 μm.

DISCUSSION

Chang [7] has reported that rabbit sperm collected from the oviduct lose the ability to fertilize following exposure to bull, human, or its own seminal plasma. He suggested that the decapacitation factor present in seminal plasma is conserved among several species, although this factor has not been identified. In this study, we report that mouse SVS2, which is a member of the semen-clotting protein family, serves as a decapacitation factor. Furthermore, human SEMG, which belongs to the semen-clotting protein family, also exhibits an inhibitory effect on sperm capacitation [23]. Our study is the first to identify and report a decapacitation factor that is conserved across species.

Some studies have already been performed on the mouse decapacitation factor. Two research groups have isolated a decapacitation factor from uncapacitated epididymal sperm; one group identified it as a 40-kDa glycoprotein [12], while the other group identified it as phosphatidylethanolamine-binding protein 1 [14]. On the other hand, Huang and colleagues [33, 34] have reported that a 19-kDa glycoprotein that is secreted from the seminal vesicle and binds to sperm phospholipids functions as a decapacitation factor. However, these studies have examined only the effects of decapacitation factor(s) on fertility in vitro using epididymal sperm. We examined the inhibitory effect of SVS2 using both in vivo and in vitro assays. Thus, we believe that SVS2 is a physiological decapacitation factor for mouse sperm.

Figure 7 shows a model of SVS2 and sperm in the female reproductive tract after copulation. Using this model, we illustrate the changes in the SVS2-binding pattern and the capacitation status of sperm in transit in the female reproductive tract. During mouse copulation, the ejaculated semen enters directly into the uterus, and the copulatory plug, which consists of SVS2, occupies the vaginal space. In the vagina, we found a few sperm that had no motility and that did not interact

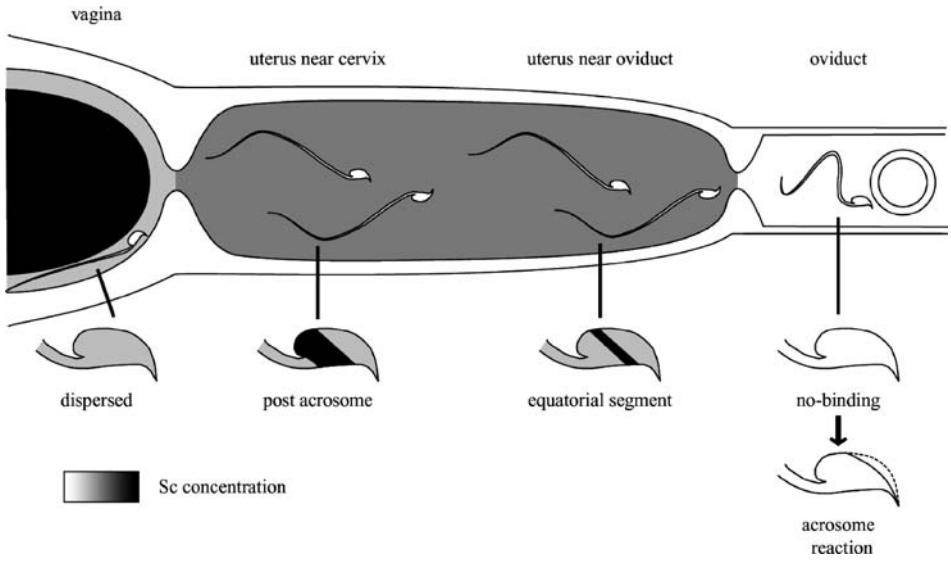

FIG. 7. Model showing SVS2 and sperm in the female reproductive tract after copulation. After copulation, most of the SVS2 forms a copulatory plug, and a small amount of SVS2 enters the uterus along with the ejaculated sperm. Although the ejaculated sperm in the vagina are not motile and do not interact with SVS2, motile sperm in the uterus show a unique pattern of SVS2 binding. While the ejaculated sperm migrate to the oviduct, the SVS2-binding region changes from the postacrosomal region to the equatorial segment. In the oviduct, which is the site of fertilization, SVS2 is rarely detected, and it does not interact with the sperm. The sperm in the oviduct can induce the acrosome reaction, while those in the vagina and uterus cannot. SVS2 functions as a decapacitation factor and inhibits the sperm acrosome reaction until the sperm reach the oocytes.

with SVS2, which suggests that the sperm may die before they interact with SVS2, and are subsequently excreted from the vagina. On the other hand, a small amount of SVS2 enters the uterus and interacts with motile sperm. When the sperm migrate from the cervix to the oviduct, the SVS2-binding pattern shows alteration from the postacrosomal region to the equatorial segment. Finally, the binding region disappears completely in sperm collected from the oviduct. Concomitant with the disappearance of the SVS2-binding activity of sperm, the sperm in the oviduct can undergo the acrosome reaction. These findings indicate that SVS2 suppresses the sperm acrosome reaction in the uterus by interacting with the sperm head. Moreover, it is known that the use of seminal plasma as a medium for artificial insemination appears to be beneficial in terms of both the motility and fertility of sperm [35]. These findings suggest that the decapacitation factor SVS2 plays a physiological role in the uterus by suppressing capacitation and the acrosome reaction in ejaculated sperm, thereby improving the fertilization rate in the oviduct.

The results of our experiments using in vivo sperm show some differences compared to those of previous studies, since most of the previous studies on sperm capacitation and decapacitation used epididymal sperm that were treated in vitro. In the present study, the SVS2-binding region of the ejaculated sperm was changed during the migration of the sperm from the cervix to the oviduct. In the uterus, the SVS2-binding pattern changed from the postacrosomal region to the equatorial segment (Fig. 7). Moreover, the sperm in the oviduct emitted weak SVS2-binding signals as compared to the negative control, i.e., epididymal sperm treated without SVS2 (Fig. 5). These changes in the SVS2-binding patterns were rarely observed in the in vitro experiments of epididymal sperm (data not shown). These results indicate that the transition of SVS2-binding patterns is not only time-dependent but also space-dependent, which suggests that some underlying mechanisms eliminate SVS2 from the ejaculated sperm surface in the female reproductive tract. Furthermore, the percentage of capacitated sperm differed between the in vivo and in vitro conditions (Fig. 4). Ejaculated sperm in the oviduct showed approximately 1.5-fold higher responsiveness to ionomycin and progesterone compared with epididymal sperm capacitated in vitro in the absence of SVS2. These results suggest that some factor in the female reproductive tract accelerates sperm capacitation. There are reports on the activation of sperm capacitation by taurine, hypotaurine [36], and glycosaminoglycan [37]. However, the in vivo functions of these factors have not been examined. Therefore, further investigations of sperm in the female reproductive tract are required to understand the mechanisms of decapacitation and capacitation of sperm.

It is well known that cholesterol efflux from the sperm membrane and increased membrane fluidity are observed during sperm capacitation [38, 39]. Membrane cholesterol is known to be a component of microdomains known as lipid rafts [40, 41], and a reduction in its content destabilizes the raft structure, thereby leading to a change in the size, distribution, and glycoprotein content of lipid rafts [42]. Some glycoproteins and gangliosides are components of lipid rafts and show variations in their distributions on the sperm surface during capacitation [43, 44]; these variations are similar to those observed for the SVS2-binding patterns of sperm (Fig. 6 and Table 1). Generally, lipid rafts affect receptor activation, membrane protein distribution, and the triggering of signaling cascades [45–48]. Recently, Bou Khalil and coworkers [49] have suggested that the binding abilities of sperm lipid rafts and the zona pellucida are increased by cholesterol efflux from sperm membranes during capacitation. Therefore, it is possible that the SVS2 receptor is located on a raft glycoprotein or ganglioside, and that SVS2 regulates the distribution and signaling cascades of these lipid rafts, thereby controlling sperm fertility.

In the female reproductive tract, SVS2 was found to be degraded into various fragments that were smaller than nSVS2 in the seminal vesicle (Fig. 1B, Fig. 2B), and it appeared that the SVS2 fragment inhibited sperm capacitation in vivo. Similar degradation has been observed for human coagulum-forming SEMG [16]. SEMG is digested by PSA secreted from the prostate, and various SEMG fragments are considered to be involved in different biological activities, such as sperm motility inhibition, inhibin-like activity, TRH-like function, and sperm coating [24, 50, 51]. Furthermore, the amino acid sequence of mouse SVS2 shows many predicted cleavage sites for PSA, and our preliminary experiment showed that human PSA could digest SVS2 in vitro (data not shown). These findings suggest that the in vivo degradation of SVS2 is caused by a PSA-like protease, and that one of the SVS2 fragments acts as a decapacitation domain. Moreover, the locations of the PSA cleavage sites on SVS2 remain unknown, since the molecular sizes of the SVS2 fragments in vivo were not sufficiently small to allow cleavage at all cleavage sites. More

precise investigations that focus on the SVS2 functional domain are required to obtain more detailed information regarding the inhibitory mechanisms of SVS2.

ACKNOWLEDGMENTS

We thank Dr. K. Miyado for valuable advice on the in vitro fertilization assay and Dr. K. Yoshida for helpful discussion.

REFERENCES

1. Chang MC. Fertilizing capacity of spermatozoa deposited into the fallopian tubes. Nature 1951; 168:697–698.
2. Austin CR. Observations on the penetration of the sperm into the mammalian egg. Aust J Sci Res 1951; (B)4:581–596.
3. DasGupta S, Mills CL, Fraser LR. Ca(2+)-related changes in the capacitation state of human spermatozoa assessed by a chlortetracycline fluorescence assay. J Reprod Fertil 1993; 99:135–143.
4. Yanagimachi R. Mammalian fertilization. In: Knobil E, Neil JD (eds.), The Physiology of Reproduction. New York: Raven Press; 1994:189–317.
5. Visconti PE, Bailey JL, Moore GD, Pan D, Olds-Clarke P, Kopf GS. Capacitation of mouse spermatozoa. II. Correlation between the capacitation state and protein tyrosine phosphorylation. Development 1995; 121:1129–1137.
6. Baker MA, Hetherington L, Ecroyd H, Roman SD, Aitken RJ. Analysis of the mechanism by which calcium negatively regulates the tyrosine phosphorylation cascade associated with sperm capacitation. J Cell Sci 2004; 117(Pt 2):211–222.
7. Chang MC. A detrimental effect of seminal plasma on the fertilizing capacity of sperm. Nature 1957; 179:258–259.
8. Bedford JM, Chang MC. Removal of decapacitation factor from seminal plasma by high-speed centrifugation. Am J Physiol 1962; 202:179–181.
9. McRorie RA, Williams WL. Biochemistry of mammalian fertilization. Annu Rev Biochem 1974; 43:777–803.
10. Davis BK. Inhibition of fertilizing capacity in mammalian spermatozoa by natural and synthetic vesicles. In: Kabara JJ (ed.), Symposium on the Pharmacological Effect of Lipids. Champaign, Illinois: The American Oil Chemists Society; 1978:145–157.
11. Oliphant G, Reynolds AB, Thomas TS. Sperm surface components involved in the control of the acrosome reaction. Am J Anat 1985; 174: 269–284.
12. Fraser LR. Interactions between a decapacitation factor and mouse spermatozoa appear to involve fucose residues and a GPI-anchored receptor. Mol Reprod Dev 1998; 51:193–202.
13. Huang YH, Kuo SP, Lin MH, Shih CM, Chu ST, Wei CC, Wu TJ, Chen YH. Signals of seminal vesicle autoantigen suppresses bovine serum albumin-induced capacitation in mouse sperm. Biochem Biophys Res Commun 2005; 338:1564–1571.
14. Nixon B, MacIntyre DA, Mitchell LA, Gibbs GM, O'Bryan M, Aitken RJ. The identification of mouse sperm-surface-associated proteins and characterization of their ability to act as decapacitation factors. Biol Reprod 2006; 74:275–287.
15. Williams-Ashman HG. Transglutaminases and the clotting of mammalian seminal fluids. Mol Cell Biochem 1984; 58:51–61.
16. Lilja H, Abrahamsson PA, Lundwall A. Semenogelin, the predominant protein in human semen. Primary structure and identification of closely related proteins in the male accessory sex glands and on the spermatozoa. J Biol Chem 1989; 264:1894–1900.
17. Dorus S, Evans PD, Wyckoff GJ, Choi SS, Lahn BT. Rate of molecular evolution of the seminal protein gene SEMG2 correlates with levels of female promiscuity. Nat Genet 2004; 36:1326–1329.
18. Lundwall A. The cloning of a rapidly evolving seminal-vesicle-transcribed gene encoding the major clot-forming protein of mouse semen. Eur J Biochem 1996; 235:424–430.
19. Harris SE, Harris MA, Johnson CM, Bean MF, Dodd JG, Matusik RJ, Carr SA, Crabb JW. Structural characterization of the rat seminal vesicle secretion II protein and gene. J Biol Chem 1990; 265:9896–9903.
20. Iwamoto T, Tanaka H, Osada T, Shinagawa T, Osamura Y, Gagnon C. Origin of a sperm motility inhibitor from boar seminal plasma. Mol Reprod Dev 1993; 36:475–481.
21. Iwamoto T, Hiroaki H, Furuichi Y, Wada K, Satoh M, Osada T. Cloning of boar SPMI gene which is expressed specifically in seminal vesicle and codes for a sperm motility inhibitor protein. FEBS Lett 1995; 368:420–424.
22. Dostalova Z, Calvete JJ, Topfer-Petersen E. Interaction of non-aggregated boar AWN-1 and AQN-3 with phospholipid matrices. A model for coating of sperm adhesins to the sperm surface. Biol Chem Hoppe Seyler 1995; 376:237–242.
23. de Lamirande E, Yoshida K, Yoshiike TM, Iwamoto T, Gagnon C. Semenogelin, the main protein of semen coagulum, inhibits human sperm capacitation by interfering with the superoxide anion generated during this process. J Androl 2001; 22:672–679.
24. Yoshida K, Yamasaki T, Yoshiike M, Takano S, Sato I, Iwamoto T. Quantification of seminal plasma motility inhibitor/semenogelin in human seminal plasma. J Androl 2003; 24:878–884.
25. Fukami K, Yoshida M, Inoue T, Kurokawa M, Fissore RA, Yoshida N, Mikoshiba K, Takenawa T. Phospholipase Cdelta4 is required for Ca2+ mobilization essential for acrosome reaction in sperm. J Cell Biol 2003; 161:79–88.
26. Huynh K, Jones G, Thouas G, Britt KL, Simpson ER, Jones ME. Estrogen is not directly required for oocyte developmental competence. Biol Reprod 2004; 70:1263–1269.
27. Kawano N, Shimada M, Terada T. Motility and penetration competence of frozen-thawed miniature pig spermatozoa are substantially altered by exposure to seminal plasma before freezing. Theriogenology 2003; 61: 351–364.
28. Amelar RD. Coagulation, liquefaction and viscosity of human semen. J Urol 1962; 87:187–190.
29. Benoff S, Barcia M, Hurley IR, Cooper GW, Mandel FS, Heyner S, Garside WT, Gilbert BR, Hershlag A. Classification of male factor infertility relevant to *in vitro* fertilization insemination strategies using mannose ligands, acrosome status and anti-cytoskeletal antibodies. Hum Reprod 1996; 11:1905–1918.
30. Goodwin LO, Leeds NB, Hurley I, Mandel FS, Pergolizzi RG, Benoff S. Isolation and characterization of the primary structure of testis-specific L-type calcium channel: implications for contraception. Mol Hum Reprod 1997; 3:255–268.
31. Thomas P, Meizel S. An influx of extracellular calcium is required for initiation of the human sperm acrosome reaction induced by human follicular fluid. Gamete Res 1988; 20:397–411.
32. Songsasen N, Leibo SP. Live mice from cryopreserved embryos derived *in vitro* with cryopreserved ejaculated spermatozoa. Lab Anim Sci 1998; 48: 275–281.
33. Huang YH, Chu ST, Chen YH. Seminal vesicle autoantigen, a novel phospholipid-binding protein secreted from luminal epithelium of mouse seminal vesicle, exhibits the ability to suppress mouse sperm motility. Biochem J 1999; 343(Pt 1):241–248.
34. Huang YH, Chu ST, Chen YH. A seminal vesicle autoantigen of mouse is able to suppress sperm capacitation-related events stimulated by serum albumin. Biol Reprod 2000; 63:1562–1566.
35. Chang MC. Effects of heterologous seminal plasma and sperm cells on fertilizing capacity of rabbit spermatozoa. Proc Exp Biol Med 1949; 70:32.
36. Meizel S, Lui WC, Working KP, Mrsny JR. Taurine and hypotaurine: their effects on motility, capacitation and the acrosome reaction of hamster sperm in vitro and their presence in sperm and reproductive tract fluids of several mammals. Dev Growth Differ 1980; 22:483–494.
37. Wincek TJ, Parrish RF, Polakoski KL. Fertilization: a uterine glycosaminoglycan stimulates the conversion of sperm proacrosin to acrosin. Science 1979; 203:553–554.
38. Visconti PE, Ning X, Fornes MW, Alvarez JG, Stein P, Connors SA, Kopf GS. Cholesterol efflux-mediated signal transduction in mammalian sperm: cholesterol release signals an increase in protein tyrosine phosphorylation during mouse sperm capacitation. Dev Biol 1999; 214:429–443.
39. Cross NL. Reorganization of lipid rafts during capacitation of human sperm. Biol Reprod 2004; 71:1367–1373.
40. Edidin M. The state of lipid rafts: from model membranes to cells. Annu Rev Biophys Biomol Struct 2003; 32:257–283.
41. Foster LJ, De Hoog CL, Mann M. Unbiased quantitative proteomics of lipid rafts reveals high specificity for signaling factors. Proc Natl Acad Sci U S A 2003; 100:5813–5818.
42. Kabouridis PS, Janzen J, Magee AL, Ley SC. Cholesterol depletion disrupts lipid rafts and modulates the activity of multiple signaling pathways in T lymphocytes. Eur J Immunol 2000; 30:954–963.
43. Baker SS, Thomas M, Thaler CD. Sperm membrane dynamics assessed by changes in lectin fluorescence before and after capacitation. J Androl 2004; 25:744–751.
44. Shadan S, James PS, Howes EA, Jones R. Cholesterol efflux alters lipid raft stability and distribution during capacitation of boar spermatozoa. Biol Reprod 2004; 71:253–265.
45. Brown DA, London E. Functions of lipid rafts in biological membranes. Annu Rev Cell Dev Biol 1998; 14:111–136.
46. Brown DA, London E. Structure and function of sphingolipid- and cholesterol-rich membrane rafts. J Biol Chem 2000; 275:17221–17224.

47. Simons K, Ikonen E. Functional rafts in cell membranes. Nature 1997; 387:569–572.
48. Simons K, Toomre D. Lipid rafts and signal transduction. Nat Rev Mol Cell Biol 2000; 1:31–39.
49. Bou Khalil M, Chakrabandhu K, Xu H, Weerachatyanukul W, Buhr M, Berger T, Carmona E, Vuong N, Kumarathasan P, Wong PT, Carrier D, Tanphaichitr N. Sperm capacitation induces an increase in lipid rafts having zona pellucida binding ability and containing sulfogalactosylglycerolipid. Dev Biol 2006; 290:220–235.
50. Iwamoto T, Gagnon C. Purification and characterization of a sperm motility inhibitor in human seminal plasma. J Androl 1988; 9:377–383.
51. Robert M, Gagnon C. Semenogelin I: a coagulum forming, multifunctional seminal vesicle protein. Cell Mol Life Sci 1999; 55:944–960.